

# Reactor Characteristic Evaluation and Analysis Technologies of JFE Steel<sup>†</sup>

HIRATANI Tatsuhiko<sup>\*1</sup> NAMIKAWA Misao<sup>\*2</sup> NISHINA Yoshiaki<sup>\*3</sup>

## Abstract:

Reactor characteristic evaluation and analysis technique was constructed by JFE Steel including the design optimization simulation for the purpose of performance improvement of high frequency reactor. Based on the simulation, reactors which satisfy a given specification were designed with different core materials and core size. The validity of the simulation result was proved by physically fabricating these reactors and estimating the performance under the actual use conditions. Moreover reactor noise visualization was achieved by using a sound energy flux density system. It is possible to promote a solution suggestion of reactor to a customer by utilizing these tools.

## 1. Introduction

In power electronics circuits, high frequency reactors are one key component which plays the roles of voltage transformer and filter by accumulation/discharge of magnetic energy. As a typical example of reactor applications, Fig. 1 shows the circuit of a power conditioner for solar power and the reactor current waveform. Reactors are used under direct current or alternating current on which a high frequency ripple is superimposed<sup>1)</sup>. In order to reduce the size of reactors, a ferromagnetic core material is usually inserted in the coil. In this type of reactor, it is necessary to pay special attention to the point that magnetic saturation exists in the core material and the point that heat generation increases remarkably due to eddy currents in the core at higher frequencies. Coil heat generation also has a large influence on the design of reactors. In order to obtain an appropriate

reactor, not only evaluation of the magnetic properties of the core material, simulation techniques for predicting the reactor characteristics reflecting the desired conditions, and technology for performing characteristic evaluation and analysis by actual excitation waveform is also essential. This paper explains the outline of reactor simulation and the reactor evaluation equipment of JFE Steel, then, introduces the comparative evaluation examples of loss and noise between the same specification reactors which are fabricated with different core materials respectively.

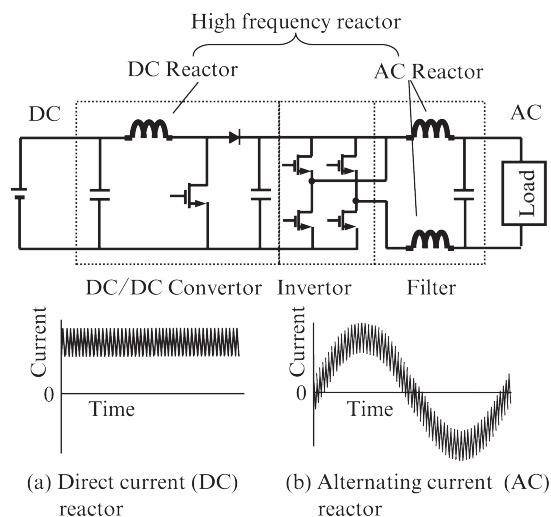


Fig. 1 Schematic diagram of basic power circuit and reactor current waveform

<sup>†</sup> Originally published in *JFE GIHO* No. 36 (Aug. 2015), p. 32–36  
“Super Core” is registered trademark of JFE Steel Corporation in Japan.



<sup>\*1</sup> Senior Researcher Manager,  
Electrical Steel Res. Dept.,  
Steel Res. Lab.,  
JFE Steel



<sup>\*2</sup> Senior Researcher Deputy General Manager,  
Numerical Simulation Res. Dept.,  
Steel Res. Lab.,  
JFE Steel



<sup>\*3</sup> Senior Researcher Deputy General Manager,  
Mechanical Engineering Res. Dept.,  
Steel Res. Lab.,  
JFE Steel

## 2. Reactor Simulation

### 2.1 Magnetic Design of Reactors

Reactor inductance  $L$  is one of the most important properties for circuit elements. Change of  $L$  due to direct current is called direct current superimposition characteristics. When electrical steel is used as the core of a reactor, direct current superimposition characteristics are adjusted by providing an air gap in the core in order to avoid sudden drops in inductance due to magnetic saturation. **Figure 2** shows the relationship between the magnetic flux density  $B$  vs. magnetizing force  $H$  curve of a core that includes a gap and its direct current superimposition characteristics. When  $N$  turns of copper wire are wound on a core with a magnetic path length  $l_m + l_g$ , which includes a gap with length  $l_g$ , and a current  $I$  is passed, if magnetic permeability in a vacuum is  $\mu_0$ , the relative permeability of the core material (differential permeability) is  $\mu_r$  and the total effective permeability of the core including the gap is  $\mu_{\text{eff}}$ , the relationship in Eq. (1) is materialized by Ampere's circuital integral law and continuity of magnetic flux.

$$\frac{B}{\mu_0 \mu_r} l_m + \frac{B}{\mu_0} l_g = \frac{B}{\mu_{\text{eff}}} (l_m + l_g) = NI \dots \dots \dots (1)$$

In case  $l_g \ll l_m$ ,  $\mu_{\text{eff}}$  can be expressed by Eq. (2).

$$\mu_{\text{eff}} = \frac{\mu_0 \mu_r}{1 + \mu_r (l_g / l_m)} \dots \dots \dots (2)$$

On the other hand, because inductance  $L$  is a value which is obtained by dividing the interlinkage flux number by current,  $L$  can be expressed as follows by using  $N$ ,  $\mu_{\text{eff}}$  and the cross-sectional area of the core  $S$ .

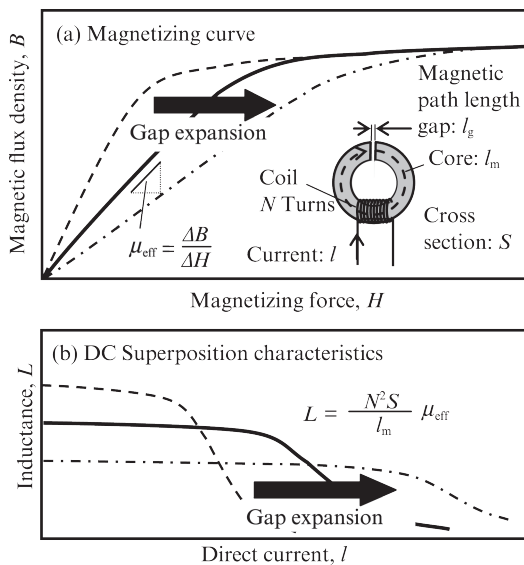


Fig. 2 Relationship between the direct current (DC) superimposition characteristics and the gap length

$$L = \frac{N^2 S}{l_m} \mu_{\text{eff}} \dots \dots \dots (3)$$

Equation (4), which expresses  $L$  by the form of the magnetic circuit, can be obtained from Eqs. (2) and (3).

$$L = N^2 \left( \frac{l_m}{\mu_0 \mu_r S} + \frac{l_g}{\mu_0 S} \right)^{-1} \dots \dots \dots (4)$$

The first term in the parentheses on the right side of Eq. (4) expresses the magnetic resistance of the core, and the second term expresses the magnetic resistance of the air gap. In cores with multiple gaps,  $L$  may be calculated by taking the sum of the magnetic resistance of each gap. As is clear from Eq. (2) and Eq. (4), as the gap length  $l_g$  is increased, the effective permeability  $\mu_{\text{eff}}$  of a core is reduced and magnetic saturation can be avoided up to the large current region; in other words, direct current superimposition characteristics are improved. As the negative aspect of this, inductance  $L$  in the service current region decreases.

The actual measured values of  $L$  are larger than the values calculated by Eq. (4), and the difference between the measured values and calculation results shows a tendency to increase with the gap length. As shown in **Fig. 3**, this is thought to be because fringing of the magnetic flux occurs in the air gaps, where permeability is low in comparison with the core material, and as a result, the cross-sectional area of the magnetic circuit increases and magnetic resistance decreases in this part. Fringing is also different depending on the shape of the gap. In order to calculate inductance with high accuracy, it is necessary to correct magnetic resistance by using the effective sectional area considering fringing of the flux for each gap shape. Therefore, assuming that the effective sectional area  $S_{gi}$  of gap shape  $i$  is a function of the gap length  $l_{gi}$ , an approximation equation is obtained experimentally by fitting to the measured data of inductance. The inductance calculation formula in this case is shown below.

$$L = N^2 \left( \frac{l_m}{\mu_0 \mu_r S} + \sum_i \frac{l_{gi}}{\mu_0 S_{gi}} \right)^{-1} \dots \dots \dots (5)$$

The direct current superimposition characteristics of a reactor can be calculated with good accuracy by using

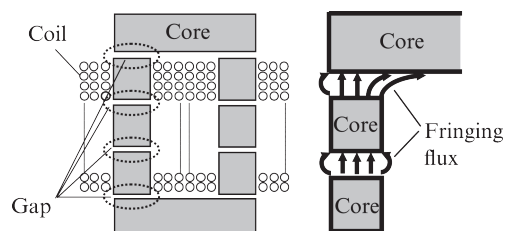


Fig. 3 Fringing flux in the gap part of reactor core

Eq. (5), which considers fringing effect of the magnetic flux, and the magnetic data for the core material (either  $\mu_r-I$  or  $\mu_r-B$  characteristics)<sup>2)</sup>.

### 2.2 Reactor Design Support

In reactor design, estimation of copper loss and core loss, which are causes of heat generation, is also important. Although various methods for calculating these types of loss have been studied<sup>3)</sup>, a simple rough calculation of loss is possible from the reactor rated current  $I_m$ , ripple amplitude  $\Delta I_{p-p}$ , direct current superimposition characteristics and iron loss characteristics of the core material. The core material, dimensions and gap length are selected so that the heat generation of the core does not exceed the allowable temperature. Similarly for the coil, the wire diameter and number of turns are adjusted considering heat generation. As shown in Eq. (5), the core sectional area and the number of turns of the coil also have a large influence on the inductance of a reactor. Moreover, even with the same number of turns, copper loss will differ depending on the coil geometry and winding method. The cooling conditions in the actual use environment, also is an important factor for the reactor design.

As described above, magnetic design, coil design and heat design are closely related. Therefore, mutually optimizing these factors so as to obtain the desired electrical specification under the given conditions can be considered the essence of a reactor design (Fig. 4).

The merits of reactor simulation include the fact that it is possible to respond flexibly, without limitations associated with evaluation equipment, for example, in predicting the characteristics of reactors which are to be used in the large current region of several hundred amperes and various control methods under excitation conditions corresponding to the power source. Moreover, simulations also make it possible to propose the most suitable use method quickly and flexibly, before manufacturing the reactor, to customers who have few opportunities to deal with electrical steel sheet.

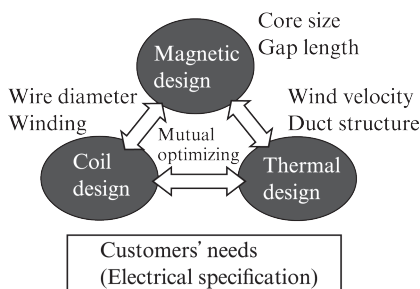


Fig. 4 Important point with a reactor design

## 3. Reactor Evaluation Equipment and Examples of Its Application

### 3.1 Reactor Evaluation Equipment

JFE Steel has introduced reactor evaluation equipment which enables magnetic excitation of reactor test materials with the specified excitation current waveform by connecting the test material and adjusting the effective value of the commercial alternating current and the frequency and amplitude of ripple, respectively, and uses this system to perform evaluation tests under a variety of conditions. The basic configuration of the reactor evaluation equipment is shown in Fig. 5. In general evaluations, ripple corresponding to the carrier frequency is superimposed on an alternating current corresponding to the rated current of the reactor, the amplitude of the ripple is adjusted while checking the waveform monitor, and the reactor loss at the specified excitation current waveform is measured with the power meter. It is also possible to measure the core loss by applying a secondary winding to the reactor. In this case, the copper loss is calculated as the difference between the reactor loss and core loss.

### 3.2 Comparison of Loss of Alternating Current Reactors

This section presents the evaluation example of an alternating current reactor which satisfies the specification in Fig. 6. As the test reactor, two test reactors were

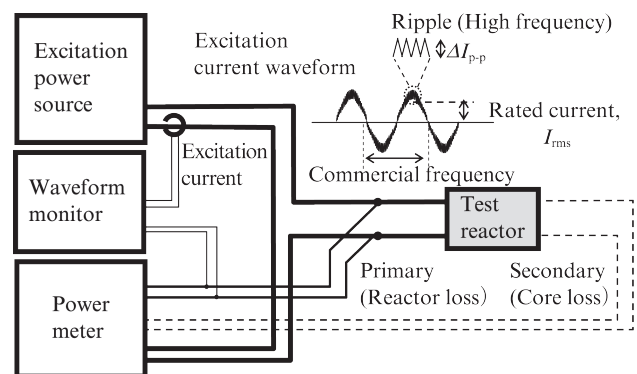


Fig. 5 Reactor evaluation equipment

#### Specifications

- Rated current: 27.5 A (50 Hz)
- Initial reactor ( $L$ ) > 850  $\mu$ H
- Rated  $L$  > 600  $\mu$ H
- Ripple current,  $\Delta I_{p-p}$ : 3.5 A
- Ripple frequency: 16 kHz

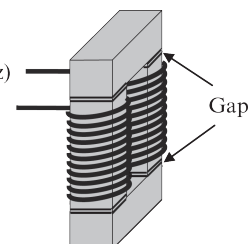


Fig. 6 Specifications of the test reactor

built using 4-block cores with dimensions of  $70 \times 20 \times 30$  mm and a coil of round copper wire, and a simulation of the number of turns of the coil and the gap length was performed for the respective cases in which [A] a Fe-Si powder core and [B] a stacked core of the high Si electrical steel Super Core™ 10JNHF600 were used as the core materials, so that approximately the same direct current superimposition characteristics were achieved in both reactors. In addition, a small-scale reactor was also built with the same core material as [B]. To secure inductance while reducing the scale of the core, it is necessary to increase the number of turns by using a smaller copper wire diameter than that in [B], but as a result, copper loss increases. Here, reactor [C], which is a small-scale version of [B], was designed in a form in which copper loss was adjusted to that in [A]. The results are shown in **Table 1**.

Evaluation reactor samples were manufactured based on the design of Table 1. **Figure 7** shows the results of measurement of their direct current superposition characteristics. The fact that all three reactors satisfy the specification in terms of both initial inductance and rated inductance can be confirmed from this figure. Next, using the reactor evaluation equipment, a loss

Table 1 Simulation results of the test reactors

Sample	[A]	[B]	[C]
Core material	Powder Core 6.5% Si-Fe	Super Core™ 10JNHF600	Super Core™ 10JNHF600
Core size (mm)	70×20×30	70×20×30	60×15×31
Gap length (mm)	0	0.7×4	0.8×4
Wire diameter (mm)	2.3φ×2	2.9φ×2	2.1φ×2
Turn number	78	58	66
Design induction, $B$ (T)	0.684	1.050	1.136
Direct current resistance (DCR) (mΩ)	24.8	12.5	25.5

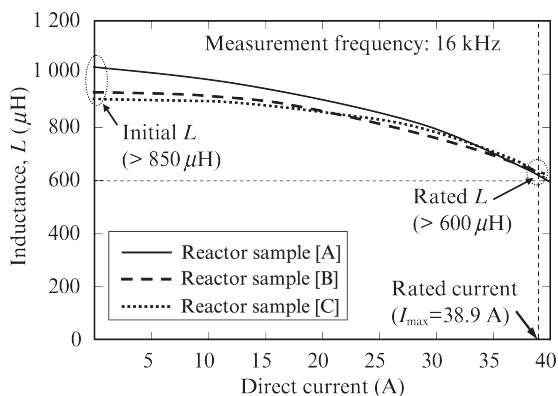


Fig. 7 Direct current (DC) superposition characteristics

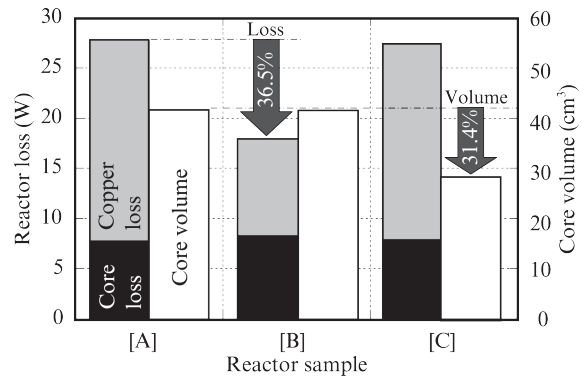


Fig. 8 Comparison of reactor losses and core volume

comparison was carried out with a waveform in which a ripple with a frequency of 16 kHz and amplitude of 3.5 A was superimposed on the rated current. With these reactors, secondary windings with the same number of turns as the respective excitation coils were wound, and core loss was measured simultaneously with reactor loss. Copper loss was obtained by subtracting core loss from reactor loss. The measurement results are shown in **Fig. 8**.

Comparing the reactor loss of [A] and [B], which have identical core dimensions, the loss of [B] was approximately 37% lower than that of [A]. When loss is separated into core loss and copper loss, it can be understood that the copper loss of [B] is small in comparison to that of [A]. This is because the effective magnetic permeability of the core material of [B] is higher than that of the powder core [A], which means the number of copper wire coil turns necessary to satisfy the inductance condition can be reduced. Next, comparing [A] and [C], in the design of [C], downsizing of the core dimensions by approximately 30% in comparison with [A] is possible while continuing to keep approximately the same copper loss. These results are in good agreement with the tendency that had been assumed when designing the specifications in Table 1. Thus, the simulation results and evaluation results show consistency.

### 3.3 Noise Evaluation of Alternating Current Reactor

Reactor noise is considered to have various causes, including magnetostrictive vibration of the core, electromagnetic force vibration of the gap, vibration of the coil, and resonance of these various types of vibration, among others. Although acoustic pressure measurements can be performed with a microphone, it is normally difficult to identify the source of reactor noise.

Recently, a system was developed and put into practical use by applying the acoustic intensity method, which makes it possible to designate the distribution of sound generated from mechanical devices and the posi-

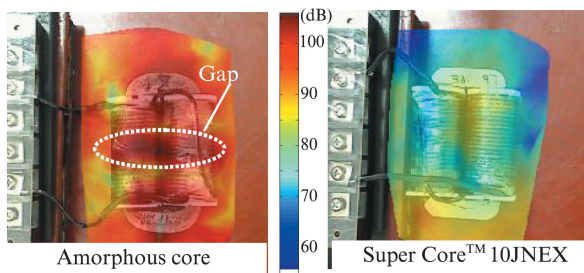


Fig. 9 Noise visualization of two reactor samples excited by same current waveform

tion of the noise source by measuring the sound energy flux<sup>4)</sup>. In this system, a microphone for acoustic pressure measurement and a particle velocity detection sensor are set in the probe, the probe is placed in front of a video camera, and the designated surface of the object is scanned. Thereafter, the track of the probe and the measurement data are matched, and the respective distributions are visualized. Visualization of the energy density is also possible by multiplying the acoustic pressure and the particle velocity.

Here, **Fig. 9** presents an example of noise visualization in which two reactors with the same specification (Rated inductance: 1.5 mH) were constructed using an amorphous cut core and a stacked core of the high Si electrical steel sheets Super Core™ 10JNEX900, respectively, and the cores were excited under conditions of a rated current of 13.6 A, ripple frequency of 10 kHz and ripple amplitude of 1.9 A.

Comparing the two cores, it can be understood that the reactor of 10JNEX900 has lower noise overall than the amorphous core. Since 10JNEX900 is a 6.5% Si electrical steel with a magnetostriction constant of close to zero, these results show that using a low magnetostriction material in the core is effective for reducing reactor noise. On the other hand, with the amorphous core, the acoustic pressure is high overall, and the level of acoustic pressure is especially high in the part corresponding to the gap of the cut core. It is estimated that the overall noise is the result of magnetostrictive vibra-

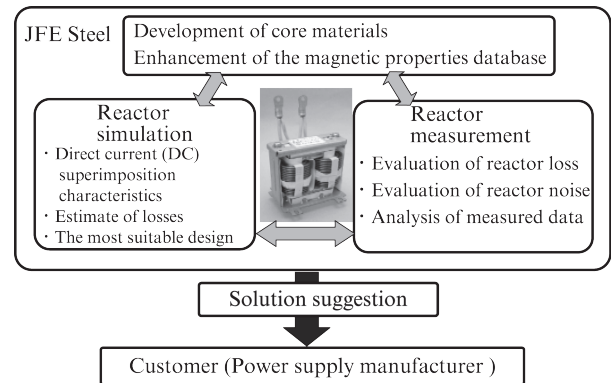


Fig. 10 Solution suggestion by reactor evaluation

tion, and the noise in the vicinity of the gap is caused by electromagnetic force. Visualization of noise in this manner is expected to enable easy designation of the noise source, and quick identification of the cause and implementation of noise reduction measures.

#### 4. Conclusion

In improving the performance of high frequency reactors, not only knowledge of soft magnetic materials and detailed data on their characteristics, but also knowledge of electrical circuits including coils and knowledge of heat, noise and vibration are necessary. JFE Steel plans to develop soft magnetic materials for use in reactor cores, and to propose quick and accurate solutions to customers by providing design support based on reactor simulations and linking measurement and analytical techniques by utilizing its reactor evaluation equipment (**Fig. 10**).

#### References

- 1) Namikawa, Misao; Ninomiya, Hironori; Yamaji, Tsunehiro. *JFE Technical Report*. 2005, no. 6, p. 12–17.
- 2) JFE Steel. Namikawa, Misao. Jpn. Registration 3709828.
- 3) Mühlethaler, J. et al. *Proceedings of the 8th International Conference on Power Electronics. ECCE Asia 2011*. p. 945–952.
- 4) de Bree, H. E. *Acoustics Australia*. 2003, vol. 31, no. 3, p. 91–94.